Development of perfluoroelastomer-based low-sorption microfluidic devices for drug metabolism and toxicity studies

2022

Mengyang Wang

TABLE OF CONTENTS

PREFACE 1
CHAPTER 1 3
I-1 INTRODUCTION 3
I-2 MATERIALS & METHODS 4
I-2.1 Fabrication of PDMS-based microfluidic devices 4
I-2.2 Fabrication of PFPE-based microfluidic devices 5
I-2.3 Isolation and primary culture of rat hepatocytes 6
I-2.4 Measurement of albumin and urea secretion 8
I-2.5 Metabolism of typical P450 (CYP) substrates 8
I-2.6 Real-time PCR 9
I-2.7 Sorption of drugs in the devices 10
I-2.8 Determination of solubility parameters of PDMS and PFPE 11
I-2.9 Statistical analyses 12
I-3 RESULTS 12
I-3.1 Hepatocyte morphology and basic functions 12
I-3.2 mRNA and functional expression of CYP enzymes 13
I-3.3 Effect of fluid flow on CYP-mediated metabolism 15
I-3.4 Sorption of drugs into PDMS and PFPE devices 18
I-3.5 Solvent swelling and solubility parameter estimation of PDMS and PFPE 19
I-4 DISCUSSION 21
I-5 SUMMARY OF CHAPTER 1 24
CHAPTER 2 25
CHAPTER 3 27
CONCLUSION 29
ACKNOWLEDGMENTS 30
REFERENCES 32

PREFACE

Recently, increasing attention has been paid to microphysiological systems (MPS). These systems incorporate microfluidics, microengineering, and biomimetic theories to fabricate artificial bioreactors that aim to simulate the essential functions of human organs in a small volume [1]. Compared to conventional static cell culture, microphysiological systems provide more physiologically relevant conditions. Perfusion culture can be utilized to provide nutrients and oxygen to the cells and to remove metabolic wastes from their surface [2]. Biochemical and biomechanical stimuli given by the system provide an in-vivo like microenvironment and allow to improve the function of the cells [3]. In addition, co-culture with different organs or tissues on the multi-organs-on-a-chip could be used to simulate the complicated structures, microenvironments, and physiology of the human body.

The liver is a complex, multi-functional organ that plays a vital part in the synthesis, metabolism, storage, filtration, and removal of important substances in the body. Several in vitro liver systems have been designed to replicate liver function and pathology. Among them, a number of liver-on-a-chip have been developed for the research of drug development, personalized medicine, disease mechanisms, and drug organogenesis [4]. However, there are still some challenges in the current research. Currently, polydimethylsiloxane (PDMS) is mainly used to fabricate microphysiological systems, but it is not suitable for drug metabolism and toxicity studies. Since most of the drugs that undergo hepatic disposition and metabolism are hydrophobic, the hydrophobic and porous nature of PDMS causes extensive absorption of these drugs [5].

To solve this problem, researchers have been exploring alternative, non-absorbent materials in the last decade [6]. Perfluoropolyether (PFPE), which has been used for sealing, coating and bonding in automotive and aerospace applications, shows a variety of unique properties, including chemical inertness and resistance to both solvents and high temperatures. In addition, it is optically transparent and biocompatible enough to be used in corneal inlays [7]. All these advantages make it possible to use PFPE as a material to fabricate a chemically repellent

microphysiological system for ADME/Tox studies.

This thesis consists of three chapters. In the first chapter, primary rat hepatocytes were cultured in the PFPE-based microfluidic device and the effect of shear stress on hepatic metabolism was investigated. Since some of the substrates used in the metabolic experiments were still absorbed by PFPE, the Hansen solubility parameter (HSP) theory was used to elucidate the mechanism of this sorption. In the second chapter, the PFPE-based microfluidic device was applied to drug toxicity studies. The liver is an important site not only for metabolism but also for detoxification, thus the feasibility of toxicity testing using this device was subsequently explored. In the final third chapter, a gut-liver-on-a-chip device was constructed to evaluate first-pass metabolism and oral bioavailability of drugs. In addition, the contribution of intestinal and liver metabolisms under the co-culture condition was also evaluated by combining pulse dosing experiments to the liver compartment inlet.

CHAPTER 1

Application of perfluoropolyether elastomers in microfluidic drug metabolism assays

I-1 INTRODUCTION

In recent years, the use of microphysiological systems for the evaluation of liver metabolism and toxicity has gained attention [8, 9]. Microphysiological systems can be considered miniature systems of artificial liver bioreactors that have been studied. Similar to bioreactors, the perfusion culture system can supply nutrients and oxygen to wash out metabolic waste [2]. Furthermore, biochemical and biomechanical stimuli given by the system improve the function of hepatocytes [3]. Once culturing begins, primary hepatocytes rapidly lose function. However, this can be mitigated with the addition of microfluidic flow. In fact, under flow conditions, albumin and urea secretion remains constant for more than 2 weeks, and gene expression of various metabolizing enzymes and transporters improved, as compared to that in static conditions [10].

Metabolism studies in microphysiological systems are hampered by the absorption of drugs into the materials used in microfabrication. Polydimethylsiloxane (PDMS) is the commonly used material because of its biocompatibility, transparency, and excellent molding characteristics, but the hydrophobic and porous nature of PDMS causes extensive absorption of hydrophobic drugs [5]. As a result, there is limited information regarding the functional presence of metabolic activity, as compared to the biological and physiological functions of hepatocytes cultured on chips. Because of the limitations of PDMS, devices using alternative, non-absorptive materials are now being explored. Recently, Campbell et al. provided an excellent review on alternative materials for the fabrication of microphysiological systems [6]. Perfluoropolyether (PFPE), like other

fluorinated polymers, is chemically inert and resistant to both solvents and high temperatures, but also has the unique characteristic of being a liquid at room temperature. PFPE has also been used as a moldable material in soft lithography. UV-curable PFPE is popular, but there is also heat-curable PFPE as well as PDMS, which can be used to fabricate multi-layered microfluidic devices [11]. In addition, PFPE is optically transparent and biocompatible enough to be used for corneal inlay.

All these advantages make it possible to use PFPE as a material to fabricate a chemically repellent liver-on-a-chip models. This chapter confirmed the sandwich culture of primary rat hepatocytes in the PFPE-based microfluidic device, then investigated the effect of hydrodynamic stimuli on albumin and urea production and drug metabolism. Furthermore, based on Hansen solubility parameter (HSP) theory, chemical repellency of PFPE in comparison with PDMS were systematically evaluated and their applicability limits were clarified.

I-2 MATERIALS & METHODS

I-2.1 Fabrication of PDMS-based microfluidic devices

The microfluidic device is composed of three parts: the upper blocks, lower blocks, and a sandwiched semipermeable membrane. The two blocks with microchannels 1 mm wide, 10 mm long, and 0.3 mm high were fabricated from PDMS using a soft lithographic technique. The positive-relief masters on silicon wafers were made by standard photolithography using the negative photoresist SU-8 2150 (MicroChem, Westborough, MA). The silicone elastomer and curing agent (Sylgard 184, Dow Corning, Midland, MI) were mixed at a volume ratio of 10:1, fully degassed, poured into the master mold, and then cured at 60 °C overnight. The PDMS slab was demolded, diced, and used to fabricate epoxy-based molds replicating the features of the SU-8 masters. After filling its channel with a small amount of epoxy resin (Epo-Tek OG142-87, Epoxy Technology, Billerica, MA), the PDMS cast was gently floated channel-side down into the

epoxy resin poured into a 60-mm aluminum dish. The epoxy resin was cured with UV irradiation for 2h, and after removal of PDMS cast, it was coated with trichloro(1H,1H,2H,2H-perfluorooctyl) silane (Sigma-Aldrich, St. Louis, MO) by vacuum deposition. The resulting epoxy resin was used as a reusable mold for device fabrication; the PDMS prepolymer was premixed as mentioned above, poured into the epoxy-based mold, and then cured at 60 °C for 6 h. Four reservoir holes were punched out with a 6-mm biopsy punch against the upper PDMS block. PDMS prepolymer, for use as a glue [12], was spread on a glass slide by spin coating at 4,000 rpm (Model K-359S1, Kyowa Riken Co., Tokyo, Japan). The upper and lower blocks were placed with the channel-side down onto the PDMS prepolymer-coated glass slide. After being left for 5 min, the blocks were detached from the glass slide. A strip-cut PETE membrane with pores of 3 μm (Sterlitech, Kent, WA) was placed on the lower block sandwiched with the upper block. Finally, the combined layers were placed at 60 °C for 6 h to cure the PDMS glue.

I-2.2 Fabrication of PFPE-based microfluidic devices

PFPE devices can be created using similar procedures as for PDMS devices. An elastomer (SIFEL X-71-8115A/B, Shin-Etsu Chemical, Japan) was mixed at the indicated ratio of 1:1, fully degassed, poured into the pre-prepared mold, and cured at 120 °C for 4 h. The following procedure was the same, except that the glass slide was spin-coated at 2,800 rpm and that the polymer glue was cured at 120 °C for 4 h. Figure 1 shows the appearance of the fabricated devices.

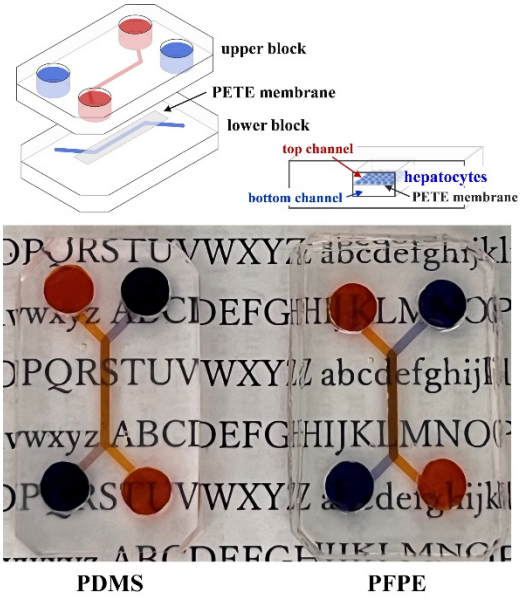

Figure 1. Structure and appearance of PDMS- and PFPE-based microfluidic devices.

I-2.3 Isolation and primary culture of rat hepatocytes

Sprague-Dawley male rats weighing 180–200 g were purchased from Japan SLC Inc., Shizuoka, Japan. All experiments were approved by the Animal Experimentation Committee of the Graduate School of Pharmaceutical Sciences, Kyoto University. A two-step collagenase perfusion method was used to isolate rat hepatocytes [13]. Rats were anesthetized with an intraperitoneal injection of a solution (10 mL/kg) consisting of 0.4 mg/mL midazolam, 0.5 mg/mL buprenorphine, and 0.03 mg/mL medetomidine. The liver was perfused with a pre-perfusion solution (115 mM NaCl, 25 mM $NaHCO_3$, 5.9 mM KCl, 1.18 mM $MgCl_2$, 1.23 mM NaH_2PO_4, and 6 mM glucose) warmed at 40 °C for 8 min, followed by 100 IU/mL of a collagenase type IV (Sigma-Aldrich, St. Louis, MO) solution (200 mL of pre-perfusion solution plus 2 mL of 10 mM $CaCl_2$) for 6 min. The rate of perfusion was set to 25 mL/min. The liver was transferred to a 10 cm plastic dish, and the serous membrane was gently torn in the Krebs-Henseleit buffer with forceps. The crude cell suspension was filtered through gauze and a 70-μm nylon mesh and centrifuged twice at 50×*g* for

3 min to remove non-parenchymal cells. The resulting hepatocytes obtained were suspended in William's E medium (Sigma-Aldrich, St. Louis, MO) supplemented with 1 mg/mL dexamethasone, 10 mg/mL amphotericin B, penicillin-streptomycin, and ITS+ premix (R&D Systems, Inc., Minneapolis, MN). Hepatocytes were used for further experiments only when their viability was > 85% after trypan blue staining.

The day before culturing, PDMS and PFPE devices were sterilized with UV irradiation for 2 h, and the upper and lower microchannels were treated with 15 μL aliquot of the coating solution (40 μL Matrigel® (Corning, Glendale, AZ) and 40 μg collagen type I (Corning) in 0.8 mL of PBS). A suspension of isolated hepatocytes (75,000 cells/15 μL) was injected into the upper microchannel of the device (Day 0). After 60 min, 200 μL of William's E culture medium was added to each of the upper and lower channel-connected wells and incubated at 37 °C in an atmosphere with 5% CO_2 in air. Six hours later, the medium was replaced with a culture medium supplemented further with 0.25 mg/mL Matrigel. After another 18 h, the culture medium was replaced with a fresh medium (Day 1). The microfluidic device was then placed on a seesaw rocking shaker (OrganoFlow®, Mimetas, Oegstgeest, The Netherlands) to initiate dynamic cell culture for a 3-min cycle with a maximum slope of 12°. The oscillation cycle was adjusted to obtain an average flow rate of 980 μL/h by measuring the volume of fluid moved during the quarter cycle. The flow rate corresponds to a shear stress of 0.15 dyne/cm^2 based on the cross-sectional shape of the microchannel [14].

Experiments were also carried out with 96-well plates. Each well was treated for 2 h at 37 °C with 100 μL of a basal culture medium containing 30 μg/mL collagen and 10 μg/mL bovine serum albumin. On day 0, hepatocytes were seeded at 50,000 cells/well onto the 96-well plates and cultured at 37 °C in an atmosphere with 5% CO_2 in air. The culture medium used and the time line for medium exchange were the same as for microfluidic devices.

I-2.4 Measurement of albumin and urea secretion

Twenty-four hours after the start of the dynamic cell culture, the culture medium was collected for measurement of secreted albumin and urea (Day 2). The measurements were performed using an Albumin ELISA kit (Bethyl Laboratories, Inc., Waltham, MA) and Urea ELISA kit (MyBioSource, Inc., San Diego, CA), respectively, according to the manufacturers' protocol.

I-2.5 Metabolism of typical P450 (CYP) substrates

On Day 2, metabolism studies were carried out in several groups. It should be noted that there were static and dynamic conditions for each of cell culture and subsequent metabolism experiment. For example, the description Flow (+/–) means that cells were cultured under dynamic conditions on Day 1 but subjected to metabolism experiment under static conditions on Day 2. The description Flow (+/+, air) means that both the cell culture and metabolism experiment were done under dynamic conditions but in the metabolism experiment the cells were exposed to air directly from the bottom by removing the lower medium. Four probe substrates were used for the metabolism studies: phenacetin (PHE, 50 μM), diclofenac (DIC, 5 μM), bufuralol (BUF, 10 μM), and midazolam (MDZ, 5 μM). The culture medium was replaced with William's E basal medium and cells were stabilized for 30 min before the onset of substrate exposure. At the onset of substrate exposure, half of the top and bottom medium were replaced with equal volumes of medium containing a two-fold concentrated cassette of each substrate. After 2 and 4 h, 100 μL of each of the top and bottom medium was collected and supplemented with an equal volume of medium containing the substrate drugs. Each sample collected was mixed with 100 μL of acetonitrile (FUJIFILM Wako Pure Chemicals, Osaka, Japan), which contained 5 μM of propranolol as an internal standard. The mixtures were filtered with a 0.45-μm pore membrane filter (Cosmonice Filter W, Nacalai Tesque, Kyoto, Japan) and analyzed by LC/MS/MS (Shimadzu LCMS-8040, Kyoto, Japan). The chromatographic separation was performed on the

XBridge C18 column (2.1 × 50 mm, 1.7 μm, Waters, Milford, CT) maintained at 40 ºC. Both the ionization mode and mobile phase are summarized in Tables 1 and 2.

Table 1. Ionization mode and multiple-reaction monitoring (MRM) transition in LC-MS/MS.

Compound	Supplier	Ionization mode	MRM transition	Collision energy
midazolam	Wako Pure Chemical	positive	326.80/292.10	−27 V
diclofenac	Tokyo Research Chemicals	positive	295.10/251.10	11 V
bufuralol	Toronto Research Chemicals	positive	262.25/188.10	16 V
phenacetin	Nacalai Tesque	positive	180.15/110.10	−23 V
1'-hydroxy midazolam	Cayman Chemical	positive	342.80/325.10	−19 V
4'-hydroxy diclofenac	Cayman Chemical	positive	313.10/231.00	−33 V
1'-hydroxy bufuralol	Toronto Research Chemicals	positive	270.05/186.10	−19 V
acetaminophen	Nacalai Tesque	positive	151.95/110.00	−18 V
propranolol (IS)	Nacalai Tesque	positive	260.35/116.15	−17 V

Table 2. HPLC conditions in LC-MS/MS.

Solvent A	0.1% formic acid	
Solvent B	0.1% formic acid-acetonitrile	
Total flow	0.2 mL/min	
B conc	10%	0−1.00 min
	10→30%	1.00−1.50 min
	30%	1.50−2.50 min
	30→95%	2.50−3.00 min
	95%	3.00−4.00 min
	95→10%	4.00−4.50 min
	10%	4.50−5.50 min
Injection volume	1 μL or 5 μL	

I-2.6 Real-time PCR

Real-time polymerase chain reactions (PCR) were used to analyze the gene expression level of rat hepatocytes. After the 24-h dynamic or static cell culture, the culture medium was removed, and the cells were washed twice with pre-warmed PBS. Then, the membrane was removed from

the device with the cells attached, transferred to a 200 μL tube, and immersed and vortexed in 70 μL of the lysis buffer supplied with the RNeasy Micro Kit (Qiagen, Hilden, Germany). Total RNA from the lysate was extracted according to the manufacturer's protocol. RNA purity and concentration were analyzed by absorbance at 260/280 nm using Nanodrop 2000 (Thermo Fisher Scientific, Waltham, MA). Ten microliter of isolated RNA solution was reversed transcribed into cDNA using the RT reagent kit (Takara Bio, Shiga, Japan), according to the manufacturer's protocol. Real-time quantitative PCR was carried out on a Step-one Sequence Detection system with a SYBR Premix (Takara Bio, Shiga, Japan). Each cycle started with a polymerase activation step for 10 min at 95 °C, followed by denaturation at 95 °C for 15 s and ended with annealing and extension at 60 °C for 60 s. Relative expression levels of target genes were calculated. GAPDH was used as a housekeeping gene. PCR primer sequences are summarized in Table 3.

Table 3. Primers used in the qPCR analysis.

GAPDH	Forward	(5'-3') AGTGCCAGCCTCGTCTCATA
	Reverse	(5'-3') GAGAAGGCAGCCCTGGTAAC
CYP3A1	Forward	(5'-3') GCCTTTTTTTGGCACTGTGCT
	Reverse	(5'-3') GCATTTGACCATCAAACAACCC
CYP3A2	Forward	(5'-3') AGTAGTGACGATTCCAACATAT
	Reverse	(5'-3') TCAGAGGTATCTGTGTTTCCT
CYP2C11	Forward	(5'-3') CGCACGGAGCTGTTTTTGTT
	Reverse	(5'-3') GCAAATGGCCAAATCCACTG
CYP2D2	Forward	(5'-3') GAAGGAGAGCTTTGGAGAGGA
	Reverse	(5'-3') AGAATTGGGATTGCGTTCAG
CYP1A2	Forward	(5'-3') TTCAGTTCAGTCCTTCC
	Reverse	(5'-3') GAAGGCTGGGAATCCATACA

I-2.7 Sorption of drugs in the devices

A cassette of four different drugs with the same concentrations as in the metabolic study were

applied to PDMS and PFPE devices without seeding the cells. Medium solutions were collected at 1, 2, and 4 h to quantitatively assess the sorption of drugs into the devices. The concentration of drugs in the collected sample aliquots was determined by LC/MS/MS as described above.

I-2.8 Determination of solubility parameters of PDMS and PFPE

PDMS and PFPE polymers were cured in 2-mm-thick sheets under the same conditions as during device fabrication and cut into 2-cm squares for swelling measurement. The sheets were immersed in 25 mL of test solvent at 25 °C for 5 days, and their weight change was measured both before and after immersion. A weight change of 6% or more was considered significant. The solvents tested were acetone, acetonitrile, benzene, chloroform, cyclohexane, cyclohexanol, diethyl ether, dimethyl formamide, dimethyl sulfoxide, 1,4-dioxane, 1,3-dioxolane, ethanol, ethyl acetate, furan, hexane, isoamyl alcohol (3-methyl-1-butanol), isopropyl ether, m-cresol, methanol, methyl ethyl ketone, methylene dichloride, n-methyl-2-pyrrolidone, pyridine, tetrahydrofuran, toluene, water, and xylene. The Hansen solubility parameters (HSPs) and sphere radii (R_o) of the cured PDMS and PFPE were determined using HSPiP Ver. 5.4.02 (https://www.hansen-solubility.com/). The HSP distance (R_a) between two materials was calculated using the following formula:

$$(R_a)^2 = 4(\delta_{D2} - \delta_{D1})^2 + (\delta_{P2} - \delta_{P1})^2 + (\delta_{H2} - \delta_{H1})^2 \quad (1)$$

where the δ_D, δ_P, and δ_H stand for the dispersion, polar, and hydrogen bonding forces, respectively, for the two materials. The relative energy difference (*RED*) between the polymers and the solvents was given as:

$$RED = R_a/R_o \quad (2)$$

Solubility parameters of the drugs were calculated by the QSAR method implemented in HSPiP.

I-2.9 Statistical analyses

Data are expressed as means ± SE from at least three independent experiments. The significance of the differences was evaluated by a one-way ANOVA test, followed by the Tukey-Kramer post-hoc test.

I-3 RESULTS

I-3.1 Hepatocyte morphology and basic functions

Primary rat hepatocytes were sandwich-cultured in the PFPE microfluidic device and stabilized in static culture for 24 h, followed by another 24 h of static or dynamic culture. Whether in static or dynamic culture, hepatocytes were similarly polygonal or cuboidal in shape and had one or two prominent nuclei. The same morphology was observed in 96-well plates (Figure 2).

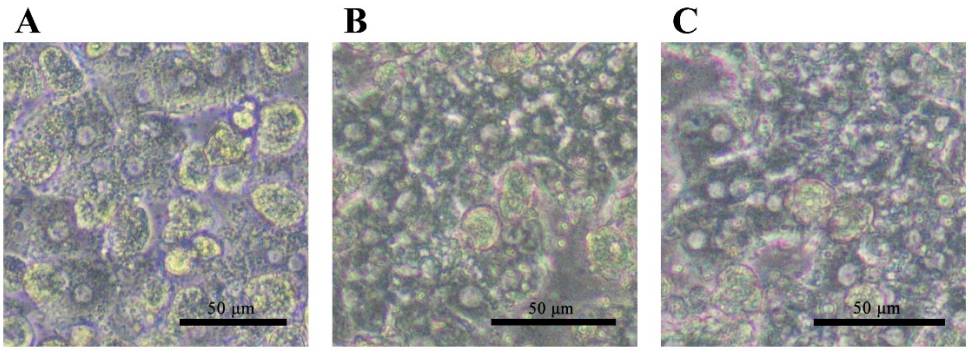

Figure 2. Microscopic observation of primary rat hepatocytes cultured in a 96-well plate (A), PFPE microfluidic devices under static conditions (B), and PFPE microfluidic devices under dynamic flow conditions (C). Scale bars indicate 50 μm.

The effect of the dynamic culture on the synthesis of albumin and urea, which are typical biochemical functional markers of hepatocytes, was also investigated in PFPE microfluidic devices (Figure 3). When albumin and urea secretion into the medium during the 24 h of static or

dynamic culturing was quantified, the dynamic culture provided 3.94-times and 1.72-times higher values than the static culture, respectively. The amount of albumin secreted was comparable between the static culture with PFPE devices and 96-well plates. The amount of urea secreted was higher in the static culture with PFPE devices. These results indicate that PFPE microfluidic devices allow for the culturing of hepatocytes equal to, or better than conventional culture plates.

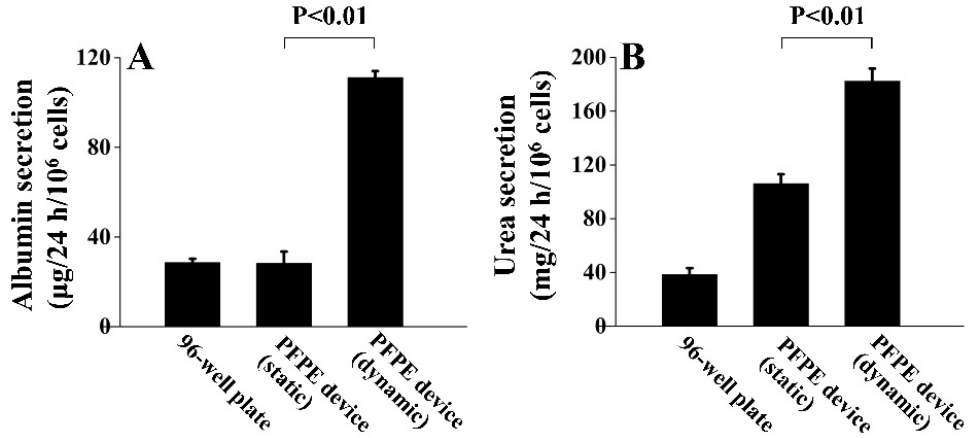

Figure 3. Secretion of albumin (A) and urea (B) from primary rat hepatocytes cultured in a 96-well plate, and PFPE microfluidic devices under static and dynamic flow conditions. The amount of albumin and urea was determined using ELISA. Data represent the mean ± SE of three samples.

I-3.2 mRNA and functional expression of CYP enzymes

The effect of dynamic culture on the expression of CYP isoforms, the major drug metabolizing enzymes in the liver, was also investigated. RT-PCR analysis showed no significant differences in gene expression of CYP isoforms between dynamic and static cultures, but gene expression for CYP1A2 and CYP2C11 tended to be slightly higher in dynamic culture (Figure 4).

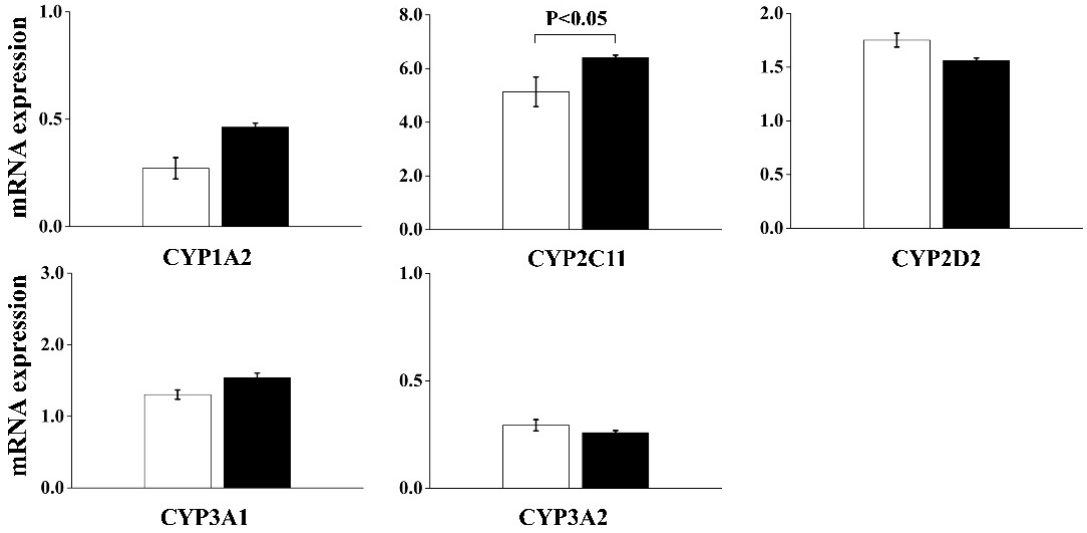

Figure 4. Gene expression of representative cytochrome P450 (CYP) isoforms in primary rat hepatocytes cultured in PFPE microfluidic devices under static (open bar) and dynamic flow (closed bar) conditions. Gene expression of each CYP was corrected by that of GAPDH, and further normalized by the relative expression in a 96-well plate. Data represent the mean ± SE of four samples.

A cocktail of four typical CYP substrates (i.e., PHE, DIC, BUF, and MDZ for CYP1A2, CYP2C11, CYP2D2, and CYP3A1/2, respectively) were applied to the hepatocytes cultured under dynamic and static conditions for 4 h. The metabolism experiments were all performed under static conditions (*i.e.*, Flow(+/–) and Flow(–/–)), so that only the effect of microfluidic flow during cell culture could be assessed. The metabolic activities for typical substrates were comparable between Flow(+/–) and Flow(–/–) conditions (Figure 5), suggesting that the dynamic culture did not significantly affect drug metabolism. Furthermore, for all the substrates, the corresponding metabolites appeared predominantly in the top chamber as opposed to the bottom chamber. It would be because the PETE membrane beneath the cells would inhibit diffusion of metabolites into the bottom chamber.

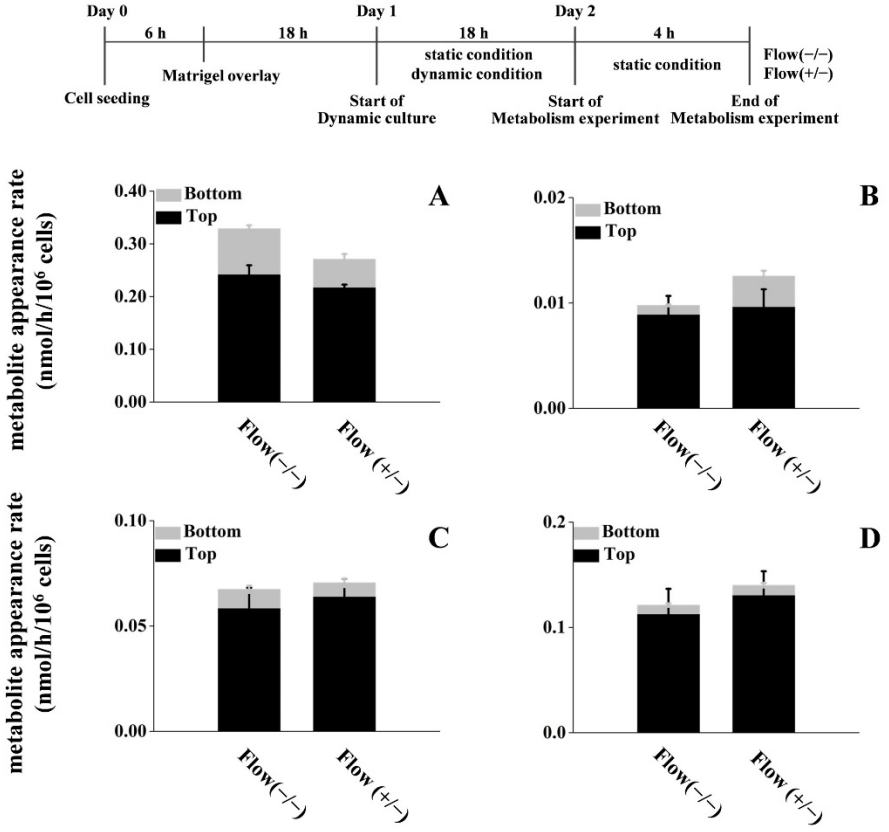

Figure 5. Metabolic activity of primary rat hepatocytes cultured in PFPE devices under static and dynamic flow conditions. All metabolism experiments were performed under static conditions to investigate the effects of dynamic flow only during the culture. The rate of appearance of metabolites in the bottom and top chambers, respectively, were calculated by linear regression of a cumulative amount data measured at 2 and 4 h after the start of the metabolism experiment. Figures 5A−D show the appearance of acetaminophen, 4'-hydroxy diclofenac, 1'-hydroxy bufuralol, and 1'-hydroxy midazolam from phenacetin (PHE), diclofenac (DIC), bufuralol (BUF), and midazolam (MDZ), respectively. Data represent the mean ± SE of four samples.

I-3.3 Effect of fluid flow on CYP-mediated metabolism

CYP-mediated metabolism is an oxygen-demanding process [15, 16], and can be affected by a dynamic oxygen supply [17]. Therefore, an investigation on the effects of the presence of

microfluidic flow on metabolic activities during metabolism was conducted (Figure 6). The metabolism of all substrates greatly increased, as compared to static conditions, with the presence of microfluidic flow. The metabolite appearance rates from PHE, DIC, BUF, and MDZ were 2.74-fold, 2.52-fold, 5.72-fold, and 6.79-fold larger, respectively. An additional experiment was conducted to confirm the extent of oxygen supply associated with microfluidic flow; that is, the medium in the bottom chamber was removed to maximize the oxygen supply to the hepatocytes. As a result, no further increase in metabolic activity was observed, demonstrating that, under this condition, the oxygen provided was sufficient to fully activate CYP450 enzymes. Even under static conditions, the bottom-side air exposure did not alter the metabolism of the substrates (Figure 7).

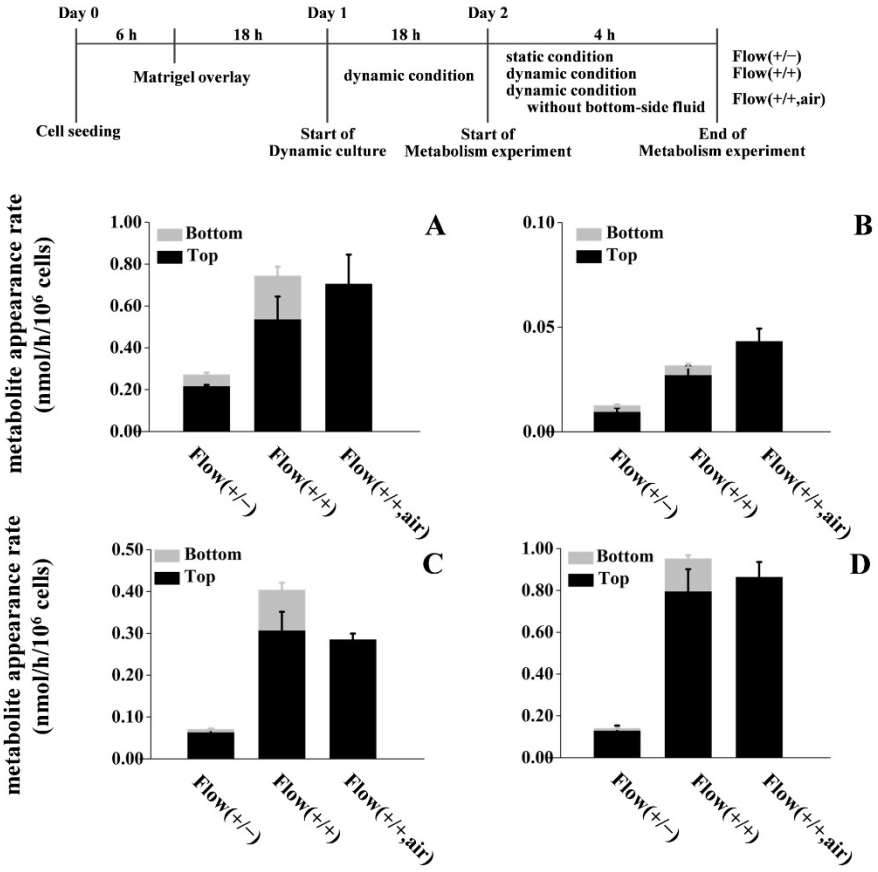

Figure 6. Effect of dynamic flow on metabolic activity of primary rat hepatocytes during metabolism experiments. All cell cultures were performed in PFPE devices under dynamic flow conditions for 24 h

before metabolism experiments. The metabolism experiments were conducted under three different flow conditions: i.e., the effect of absence (Flow(+/–)) and presence (Flow(+/+)) of dynamic flow and bottom-side air exposure (Flow(+/+,air)) were compared. The rate of appearance of metabolites in the bottom and top chambers were calculated by linear regression of a cumulative amount data measured at 2 and 4 h after the start of the metabolism experiment. Figures 6A−D show the appearance of acetaminophen, 4'-hydroxy diclofenac, 1'-hydroxy bufuralol, and 1'-hydroxy midazolam from phenacetin (PHE), diclofenac (DIC), bufuralol (BUF), and midazolam (MDZ), respectively. Data represent the mean ± SE of four samples.

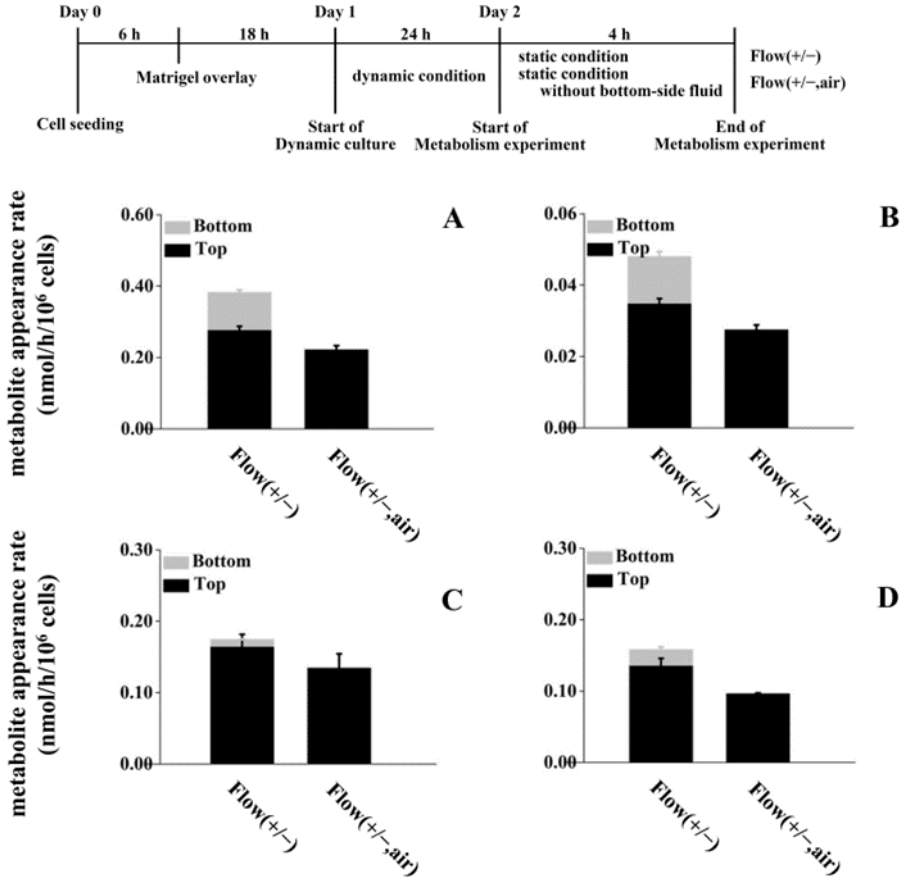

Figure 7. Effect of bottom-side air exposure on metabolic activity of primary rat hepatocytes during metabolism experiments. All cell cultures were performed in PFPE devices under dynamic flow conditions for 24 h before metabolism experiments. The metabolism experiments were conducted under static conditions, but one group was exposed directly to the air by removing the bottom-side fluid (Flow(+/–,air)). The rate of appearance of metabolites in the bottom and top chambers were calculated by linear regression

of a cumulative amount data measured at 2 and 4 h after the start of the metabolism experiment. Figures 7 A−D show the appearance of acetaminophen, 4'-hydroxy diclofenac, 1'-hydroxy bufuralol, and 1'-hydroxy midazolam from phenacetin (PHE), diclofenac (DIC), bufuralol (BUF), and midazolam (MDZ), respectively. Data represent the mean ± SE of four samples.

I-3.4 Sorption of drugs into PDMS and PFPE devices

Drug sorption into PFPE devices were compared to that into PDMS devices. A cassette of four different drugs with the same concentrations as in the metabolism study were applied to both PFPE and PDMS devices without cell seeding and measured at given time intervals. In the case of PDMS devices, the concentrations of DIC and PHE remained constant for 4 h, while the concentrations of MDZ and BUF extensively decreased over time (Figure 8). As have been well-known [6], the decrease in concentration is due to the sorption of hydrophobic drugs into PDMS devices. In PFPE devices, the sorption of MDZ was greatly reduced, but the sorption of BUF was still observed.

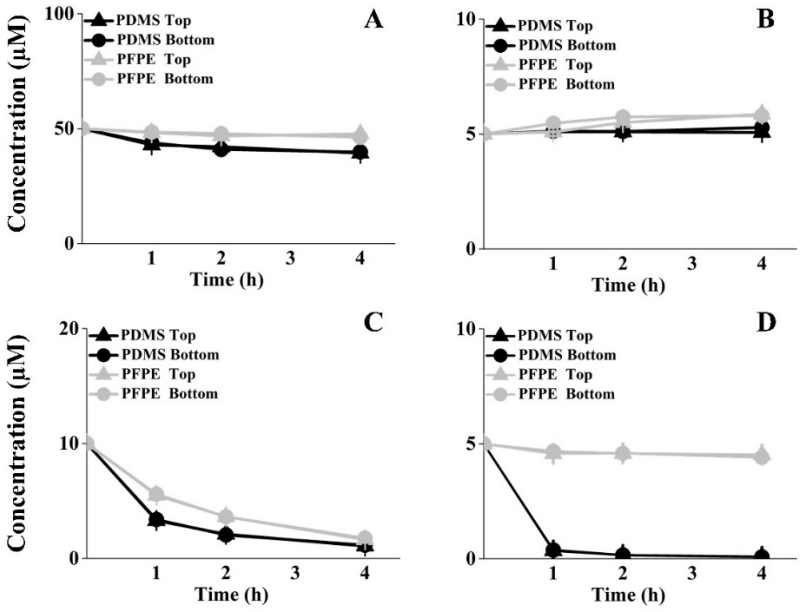

Figure 8. Time course of drugs remaining in the fluids of PDMS and PFPE devices. Drugs were

administered to the devices that had not been seeded with cells, to investigate the sorption of drugs into the device materials. The amount of drugs in both the top and bottom chambers was measured individually. Figures 8A−D show the results of phenacetin (PHE), diclofenac (DIC), bufuralol (BUF), and midazolam (MDZ), respectively. Data represent the mean ± SE of three samples.

I-3.5 Solvent swelling and solubility parameter estimation of PDMS and PFPE

Basically, swelling of polymers is induced by the sorption of solvents [18, 19]. What molecules and to what extent are absorbed by PDMS and PFPE were investigated using organic solvents with varying solubility parameters. PDMS swelled extensively in many of the solvents (Figure 9). In contrast, PFPE was much more resistant to swelling, and the degree of swelling was at most 10%.

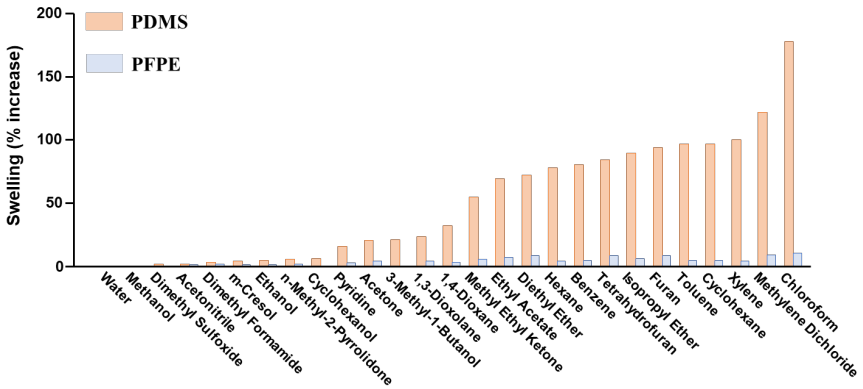

Figure 9. Swelling of PDMS and PFPE exposed to various solvents for 5 days. The degree of swelling was evaluated as a percent increase in weight relative to the original weight. Data represent the average of two samples.

The swelling characteristics of PDMS and PFPE were further analyzed using the HSP method. Hansen solubility parameters are an empirical measure that illustrates the “like dissolves like” concept, which were originally developed from the Hildebrand’s regular solution theory [20, 21].

The threshold for swelling was set at a 6 % weight increase, due to there being a large gap in PDMS swelling near that value (5.81 % (cyclohexanol) vs 15.8 % (pyridine), Figure 9). Figure 10 shows the results of the HSP analysis for PDMS and PFPE, where the coordinates at the center of the HSP spheres indicate their HSPs. It was clear that as the *RED* became greater, the degree of swelling became smaller (Figure 10, bottom). As summarized in Table 4, the HSPs were similar in both PDMS and PFPE, but the HSP radius was much smaller in PFPE. Table 4 also summarizes the solubility parameters of four drugs that have been calculated from their chemical structures with HSPiP software. Among drugs used in metabolism studies, BUF has solubility parameters that resemble those of PDMS and PFPE. The *RED*s of BUF for PDMS and PFPE were estimated to be 0.48 and 1.00, respectively, which was much smaller than those of the other three drugs. On the contrary, the *RED* for water, which reflects the escaping tendency from water, was estimated to be larger for both MDZ and BUF than for DIC and PHE.

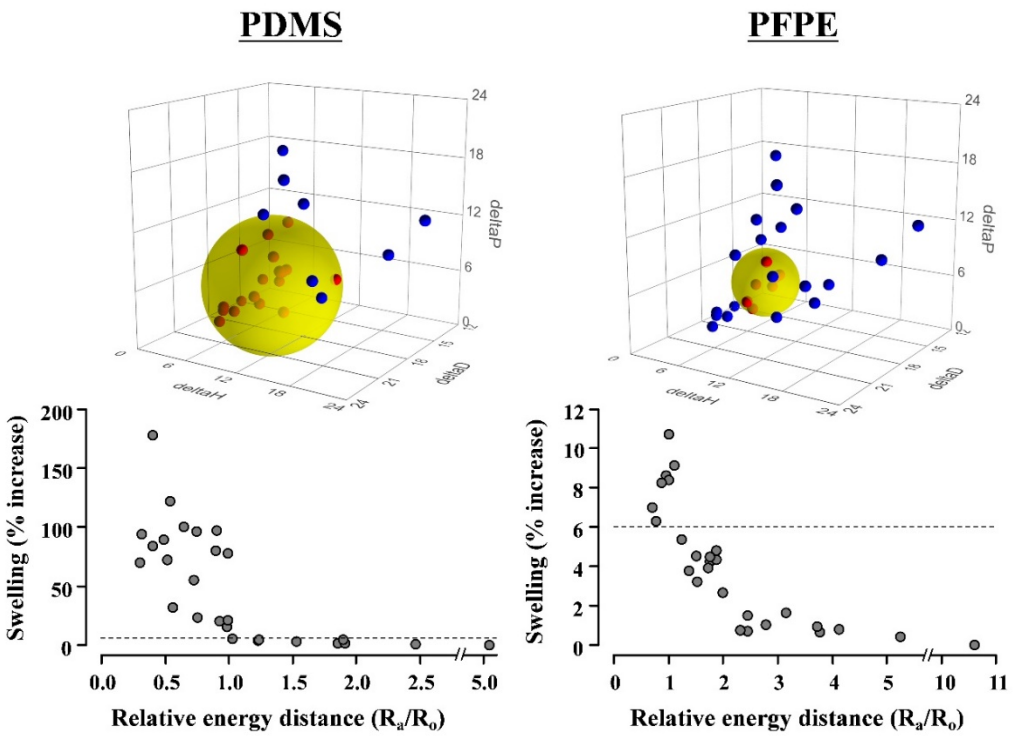

Figure 10. Hansen solubility parameter (HSP) analysis for PDMS and PFPE materials. HSP spheres were

determined from swelling against solvents with different solubility parameters. The red symbols in the top figures indicate solvents that have increased the weight of the material, due to swelling, by more than 6% of its original weight. The bottom figures show the relationship between the degree of swelling and relative energy distance (*RED*) of the solvents. The *RED*s were calculated from the HSPs of solvents using the center and radius of the HSP spheres (see Eq. 2).

Table 4. Hansen solubility parameters, molar volume, and relative energy differences.

	HSPs ($MPa^{1/2}$)			MV	HSP radius	*RED*[a)]		
	δ_D	δ_P	δ_H	(cm^3/mol)		PDMS	PFPE	Water
PDMS[b)]	16.3	3.6	6.0	—	7.6	—	—	—
PFPE[b)]	16.1	4.4	5.8	—	3.7	—	—	—
water[c)]	15.5	16.0	42.3	—	3.96	5.05	10.36	—
Phenacetin (PHE)[d)]	19.05	11.60	8.47	161.3	—	1.32	2.76	8.80
Diclofenac (DIC)[d)]	20.62	6.60	9.97	212.6	—	1.31	2.62	8.89
Bufuralol (BUF)[d)]	17.30	4.05	2.99	246.7	—	0.48	1.00	10.42
Midazolam (MDZ)[d)]	20.18	7.77	2.48	249.2	—	1.24	2.55	10.54

a) Relative energy difference (*RED*) was calculated using Eq. 2.

b) Hansen solubility parameters (HSPs) and HSP radii (R_o) of PDMS and PFPE were experimentally determined by setting the threshold for solvent swelling of the materials at a 6% weight increase.

c) HSPs and R_o of water were taken from the list of HSPiP software.

d) HSPs and molar volume (MV) of the drugs were calculated from their chemical structure by the group contribution method implemented in HSPiP software.

I-4 DISCUSSION

The liver is a highly vascularized organ that processes approximately 25–30% of total blood volume in the body [22]. The sinusoidal vessels in the liver have a diameter of 5–10 μm and blood

flows within the vessels at a shear stress of 0.1–0.5 dyne/cm^2 [23]. However, in vitro models have used a wide range of different shear stresses because direct shear stress on hepatocytes cannot be estimated. This is due to the presence of the sinusoidal endothelium and Disse's space. High shear stress in dynamic cultures adversely affects both in vitro function and hepatocyte viability [24, 25]. On the contrary, dynamic cultures allow for improved oxygen and nutrient supply, as well as the removal of waste products [2]. Since hepatocytes are metabolically active by nature, hepatocyte function can be easily impaired when cultured in narrow microchannels. Thus, there must be a trade-off in providing dynamic flow in hepatocyte culture. Under the current dynamic culture conditions (a shear stress of 0.15 dyne/cm^2; Figure 3), albumin and urea synthesis increased. Matrigel-overlaid sandwich cultures may also play a role in improving the function of hepatocytes. Sandwich cultures are generally applied to inhibit hepatocyte dedifferentiation [26]. However, sandwich cultures are also known to be effective in protecting hepatocytes from shear stress in dynamic cultures [27].

The gene expression and metabolic activity of CYPs did not differ between dynamic and static cultures. (Figures 4 and 5). Conflicting results have been reported on whether microfluidic flow upregulates the gene expression of CYPs [28-31]. Although there have also been reports that fluid-induced shear stress activates transcription factors that induce CYP expression such as pregnane X receptors (PXR) [32] and aryl hydrocarbon receptors (AhR) [33], these comparisons were made against static conditions, in which hepatocytes readily dedifferentiate. Baudoin et al [34] found that the expression of most detoxification-related genes was extensively reduced, as compared to immediately after isolation. They suggested that the appropriate time for screening is after a 24- or 48-h perfusion at optimal flow rate and cell density [34]. Since the CYP gene expression in this study was compared after 24 h of dynamic culture, the difference between static and dynamic cultures may not have been significant.

On the other hand, the metabolism of all substrates greatly increased with the presence of microfluidic flow (Figure 6). It has been well-known that CYP metabolism can be increased by

improving oxygen supply [35, 36]. However, since the bottom-side air exposure to the cells did not further improve metabolism, the effect of microfluidic flow observed in this study would not be related to oxygen supply. Conceivably, microfluidic flow could facilitate fluid mixing and delivery of drug substrates to the cells.

PFPE exhibited much stronger chemical repellency than PDMS. Swelling due to organic solvents was at most a 10% weight increase for PFPE, but as much as 100% or more for PDMS (Figure 9). This indicates a greater potential for PFPE use as a material for microfluidic devices. However, it should be noted that BUF was extensively absorbed by not only PDMS but PFPE devices (Figure 8). Drug sorption into device materials primarily occurs through physical interactions. Therefore, HSP theory was introduced to clarify which drugs are easily absorbed. HSP theory provides insight into the miscibility and solubility in solute-solvent systems by evaluating the difference in the partial cohesive energies, which consists of dispersion, polar, and hydrogen bonding forces [20, 21]. The analysis clearly demonstrated that the solvents with smaller *RED* values penetrated the materials more (Figure 10). In addition, when the HSP values were calculated from the chemical structures of the drugs, the difference in the *RED* values successfully illustrated higher sorption of BUF into PFPE. However, further consideration is needed to explain the difference in sorption into PDMS. Higher sorption of MDZ into PDMS cannot be explained in the same manner, as the *RED* values of MDZ, PHE, and DIC were nearly identical. The absorption of drugs into the device materials is a partition-diffusion process. In other words, both the interactions with materials and interactions with water should be considered. The *RED* values for water indicate that MDZ has a stronger tendency than PHE and DIC to escape from water (Table 4). Moreover, for hydrophobic drugs, “iceberg” formation makes solvation in water entropically unfavorable [37]. Therefore, MDZ, being hydrophobic and large in molecular size, would have been more readily absorbed into PDMS. Thus, the HSP approach may be useful in predicting the risk of absorption of test drugs into device materials.

I-5 SUMMARY OF CHAPTER 1

This chapter has been demonstrated that PFPE was much more chemically repellent than PDMS and primary hepatocytes could be cultured in a PFPE-based microfluidic device, thus making it possible to be used in ADME/Tox studies. Dynamic flow could enhance not only cellular functions but also CYP metabolic activity. Sorption into device materials was still problematic for certain drugs, but could be predicted by the HSP theory.

CHAPTER 2

Co-Culture of Primary Rat Hepatocytes and Non-Parenchymal Cells in Perfluoropolyether-Based Devices in Hepatotoxicity Studies

Hepatotoxicity is one of the primary causes of post-marketing drug withdrawals [38]. A number of in vitro liver models have been established to study hepatotoxicity. Researchers have usually focused only on hepatocytes [39, 40] but many non-parenchymal cells (NPCs), which have important functions, that have been overlooked. There is substantial evidence that co-culture models with hepatocytes and non-hepatocytes are more accurate in predicting hepatotoxicity than liver models with only hepatocytes, as NPCs are largely involved in the inflammation of drug induced liver injury [41, 42].

Several in vitro models have been developed to co-culture hepatocytes (PCs) and NPCs. Bale *et al.* co-cultured them on a cell culture insert with a porous membrane, i.e., Transwell, and indicated the presence of the interactions between PCs and NPCs [43]. Baze *et al.* constructed a 3D spheroid coculture system on 96-well ULA plates and confirmed that co-culture could improve hepatic functions [44]. However, these co-culture models either ignore the physiologically relevant microenvironment or are unable to emulate the physical and chemical properties of the Space of Disse. Kang *et al.* have presented a groundbreaking study of reconstituting liver sinusoids on a PDMS-based device with dual-channel configuration [45]. The two microchannels

were separated by a porous membrane that mimics liver sinusoids. Primary rat PCs were seeded into one channel, and a non-liver endothelial cell line was seeded into the other channel. With continuous perfusion, the hepatocytes maintained their normal morphology and continued to produce urea for at least one month. In addition, the dual-channel configuration also allows cells to be isolated from each channel for analyzing cell function without contamination from other cell types. Nevertheless, few studies have been conducted to study drug-induced hepatotoxicity by simulating liver sinusoid on microphysiological systems.

In this chapter, the PFPE-based devices were used to co-culture primary rat hepatocytes and non-parenchymal cells on upper and lower microchannels separately, followed by exposure to hepatotoxicants, i.e., acetaminophen (APAP) and coumarin (COU). Co-culture with non-parenchymal cells improved the viability of hepatocytes, and reduced the release of ALT/AST into the medium following the 48-h exposure to hepatotoxicants. Moreover, co-culture with non-parenchymal cells restored the level of reduced-form glutathione due to the hepatotoxicants, and alleviated the oxidative stress caused by acetaminophen. In addition, co-culture with non-parenchymal cells elevated the glutathione conjugate of acetaminophen, and reduced the level of o-hydroxyphenylacetic acid, a product from the toxic metabolite (o-hydroxyphenylacetaldehyde) of coumarin. These results suggest that non-parenchymal cells could protect against drug-induced liver injury. Thus, the two-channel microfluidic devices could also be used to assess hepatotoxicity, which would account for cell-cell interactions in the liver.

CHAPTER 3

Perfluoropolyether-Based Gut-Liver-on-a-chip Device for the Evaluation of Oral Drug Bioavailability

Oral administration is the primary route of administration because of its simplicity and inexpensiveness. Orally administered drugs are absorbed from the small intestine and delivered to the liver via the portal vein. These permeability and metabolism barriers limit the fraction of drug entering the systemic circulation, so-called oral bioavailability. Assessment of the oral bioavailability of drugs is thus critical for predicting their efficacy and safety.

In silico, in vitro, and in vivo animal models have been extensively being studied to predict oral bioavailability of drugs [46-48]. Because animal models are subject to issues of animal welfare and species differences, the combination of appropriate physiologically based pharmacokinetic models with in vitro experimental measurements such as cell permeability and hepatocyte metabolism is often used to make predictions. However, conventional planar cell cultures only allow one type of cells to be cultured in a dish and cannot deal with the interactions between organs [49]. For example, fibroblast growth factor 15/19, which is produced by the gut, is known to be involved in the synthesis of bile acids in the liver [50]. A co-culture model might be of use to account for communications between different organs. Multiorgan-on-a-chip consists of separate chambers connected by microfluidic channels, providing a method for monitoring the

dynamic responses of multiple organs to pharmaceutical agents [51].

In this chapter, a gut-liver-on-a-chip system was constructed. Midazolam that had penetrated the epithelial layer are transported to the hepatocyte compartment by sub-epithelial microchannel fluid flow. By measuring the outflow samples from the liver compartment, first-pass metabolism and bioavailability were evaluated. In addition, the intestinal and hepatic metabolic processes were assessed separately by combining pulse dosing experiments to the liver compartment inlet. Upon the assessment and analysis techniques developed, pharmacokinetic drug-drug interaction following oral administration of perpetrator and victim drugs was also evaluated by using the microfluidic gut-liver-on-a-chip device.

After midazolam was administered on the apical side of the gut chamber, both intact and metabolite forms were detected in the effluent from the liver chamber. However, extensive sorption of midazolam was observed in PDMS-based devices. Experiments using PFPE-based devices indicated that the rate of appearance of the metabolite was dose-dependent for midazolam and was also significantly suppressed by concomitant administration of ketoconazole. When genome-edited CYP3A4/UGT1A1-expressing Caco-2 cells were used, metabolites of midazolam appeared in the apical fluid. Taken together with the data on midazolam injected into the liver, it was clear that most of the metabolites of midazolam produced in the intestinal compartment were secreted into the apical fluid. While further improvements in absolute prediction of human bioavailability are needed, the gut-liver-on-a-chip device should allow for a basic assessment of saturation pharmacokinetics and drug-drug interactions for oral drugs.

CONCLUSION

PFPE elastomers have been demonstrated to ameliorate the significant sorption problems encountered in PDMS-based organs-on-a-chip devices; PFPE-based microfluidic devices have not lost the fundamental properties of PDMS in manufacturing and functional evaluation. These findings contribute to the development of microphysiological systems intended for in vitro ADMET studies.

ACKNOWLEDGMENTS

First of all, I would like to thank Professor Fumiyoshi Yamashita, Department of Drug Delivery Research, Graduate School of Pharmaceutical Sciences, Kyoto University for accepting me as a student and giving me the chance to Japan to study in his lab with so many great people. I would like to thank him for his careful guidance and supervision, which enabled me to expand my knowledge base in three and a half years.

Then, I would like to express my gratitude to Associate Professor Yuriko Higuchi, Department of Drug Delivery Research. Dr. Higuchi helped me a lot during the preliminary stage of my research, and without her guidance, my experiments might not have progressed as smoothly. In addition to my research, Dr. Higuchi also helped me a lot in living when I first came here, so that I could adapt to life in Japan quickly.

I would like to thank Junior Associate Professor Kazuo Takayama, Center for iPS Cell Research and Application (CiRA), Kyoto University, and Associate Professor Yu-suke Torisawa, Department of Micro Engineering, Kyoto University, for their technical guidance on device fabrication and perceptive comments on Chapter 1. I would like to thank Ms. Sayaka Deguchi from Center for iPS Cell Research and Application (CiRA), Kyoto University for her timely communication on the progress of the experiments and comments on Chapter 1.

I would like to extend my thanks to Professor Ryuji Yokokawa and Dr. Ryohei Ueno, Department of Micro Engineering, Graduate School of Engineering, Kyoto University, for providing the master mold for fabricating the devices.

I would like to extend my thanks to Assistant Professor Ryosuke Negoro, Laboratory of Molecular Pharmacokinetics, College of Pharmaceutical Sciences, Ritsumeikan University, for providing CYP3A4-POR-UGT1A1-KI Caco-2 cells.

I would like to thank Senior Assistant Professor Masahiro Tsuda and Assistant Professor Kanako So, Department of Applied Pharmaceutics and Pharmacokinetics, Graduate School of Pharmaceutical Sciences, Kyoto University for their valuable discussion and helpful advice.

I would like to thank everyone in the Department of Drug Delivery Research and Department of Applied Pharmaceutics and Pharmacokinetics, both alumni and current members, for their assistance with life and experiments, as well as the wonderful memories shared over the last three and a half years. I would like to express my heartfelt gratitude to Mr. Hirotaka Tatsuoka for providing technical guidance for fabricating the PFPE-based devices, Ms. Yuko Sasaki for providing technical guidance for cell culture and RT-PCR experiments, Mr. Mizuki Uno and Mr. Kazuma Aoki for helping me to establish the LCMS assay method.

I would like to thank the China Scholarship Council for supporting me during these three years, so that I can focus on my research.

Finally, I would like to thank my family for showing me the beauty of the world and educating me to be a responsible person and to be able to face the world independently. Thank you for your silent dedication. It is with your love that I can fearlessly chase my dreams.

REFERENCES

[1] F. Zheng, F. Fu, Y. Cheng, C. Wang, Y. Zhao, Z. Gu, Organ-on-a-Chip Systems: Microengineering to Biomimic Living Systems, Small 12(17) (2016) 2253-82.

[2] C.H. Beckwitt, A.M. Clark, S. Wheeler, D.L. Taylor, D.B. Stolz, L. Griffith, A. Wells, Liver 'organ on a chip', Exp Cell Res 363(1) (2018) 15-25.

[3] K. Tan, P. Keegan, M. Rogers, M. Lu, J.R. Gosset, J. Charest, S.S. Bale, A high-throughput microfluidic microphysiological system (PREDICT-96) to recapitulate hepatocyte function in dynamic, re-circulating flow conditions, Lab Chip 19(9) (2019) 1556-1566.

[4] E. Moradi, S. Jalili-Firoozinezhad, M. Solati-Hashjin, Microfluidic organ-on-a-chip models of human liver tissue, Acta biomaterialia 116 (2020) 67-83.

[5] M.W. Toepke, D.J. Beebe, PDMS absorption of small molecules and consequences in microfluidic applications, Lab Chip 6(12) (2006) 1484-6.

[6] S.B. Campbell, Q. Wu, J. Yazbeck, C. Liu, S. Okhovatian, M. Radisic, Beyond Polydimethylsiloxane: Alternative Materials for Fabrication of Organ-on-a-Chip Devices and Microphysiological Systems, ACS Biomater Sci Eng 7(7) (2021) 2880-2899.

[7] R.Z. Xie, M.D. Evans, B. Bojarski, T.C. Hughes, G.Y. Chan, X. Nguyen, J.S. Wilkie, K.M. McLean, A. Vannas, D.F. Sweeney, Two-year preclinical testing of perfluoropolyether polymer as a corneal inlay, Investigative ophthalmology & visual science 47(2) (2006) 574-581.

[8] D. Liu, S. Jiao, J. Wei, X. Zhang, Y. Pei, Z. Pei, J. Li, Y. Du, Investigation of absorption, metabolism and toxicity of ginsenosides compound K based on human organ chips, International Journal of Pharmaceutics 587 (2020).

[9] Q. Ramadan, M. Zourob, Organ-on-a-chip engineering: Toward bridging the gap between lab and industry, Biomicrofluidics 14(4) (2020) 041501.

[10] R. Jellali, T. Bricks, S. Jacques, M.J. Fleury, P. Paullier, F. Merlier, E. Leclerc, Long-term human primary hepatocyte cultures in a microfluidic liver biochip show maintenance of mRNA levels and higher drug metabolism compared with Petri cultures, Biopharm Drug Dispos 37(5) (2016) 264-75.

[11] N.S. Devaraju, M.A. Unger, Multilayer soft lithography of perfluoropolyether based elastomer for microfluidic device fabrication, Lab Chip 11(11) (2011) 1962-7.

[12] B.H. Chueh, D. Huh, C.R. Kyrtsos, T. Houssin, N. Futai, S. Takayama, Leakage-free bonding of porous membranes into layered microfluidic array systems, Anal Chem 79(9) (2007) 3504-8.

[13] B.L. Kreamer, J.L. Staecker, N. Sawada, G.L. Sattler, M.T. Hsia, H.C. Pitot, Use of a low-speed, iso-density percoll centrifugation method to increase the viability of isolated rat hepatocyte preparations, In Vitro Cell Dev Biol 22(4) (1986) 201-11.

[14] L. Kim, Y.-C. Toh, J. Voldman, H. Yu, A practical guide to microfluidic perfusion culture of adherent mammalian cells, Lab on a Chip 7(6) (2007) 681-694.

[15] E.H. Gilglioni, J.C. Chang, S. Duijst, S. Go, A.A.A. Adam, R. Hoekstra, A.J. Verhoeven, E.L. Ishii-Iwamoto, R.P.J. Oude Elferink, Improved oxygenation dramatically alters metabolism and gene expression in cultured primary mouse hepatocytes, Hepatol Commun 2(3) (2018) 299-312.

[16] U.M. Zanger, M. Schwab, Cytochrome P450 enzymes in drug metabolism: regulation of gene expression, enzyme activities, and impact of genetic variation, Pharmacol Ther 138(1) (2013) 103-41.

[17] M. Tehranirokh, A.Z. Kouzani, P.S. Francis, J.R. Kanwar, Microfluidic devices for cell cultivation and proliferation, Biomicrofluidics 7(5) (2013) 51502.
[18] D.J. Buckley, M. Berger, The swelling of polymer systems in solvents. II. Mathematics of diffusion, Journal of Polymer Science 56(163) (1962) 175-188.
[19] D. Buckley, M. Berger, The swelling of polymer solvents. III. Sorption of liquids by elastomers, Journal of Polymer Science 58(166) (1962) 1141-1152.
[20] Hansen, Charles, Hansen Solubility Parameters (A User¥"s Handbook, Second Edition) || Table A.2, 10.1201/9781420006834 (2007) 485-505.
[21] C.M. Hansen, The Universality of Solubility Parameter, Industrial & Engineering Chemistry Product Research and Development 8(1) (1969).
[22] S.E. Bradley, F.J. Ingelfinger, G.P. Bradley, J.J. Curry, The Estimation of Hepatic Blood Flow in Man, J Clin Invest 24(6) (1945) 890-7.
[23] P.F. Lalor, D.H. Adams, Adhesion of lymphocytes to hepatic endothelium, Mol Pathol 52(4) (1999) 214-9.
[24] Y. Tanaka, M. Yamato, T. Okano, T. Kitamori, K. Sato, Evaluation of effects of shear stress on hepatocytes by a microchip-based system, Measurement Science and Technology 17(12) (2006) 3167-3170.
[25] A.W. Tilles, H. Baskaran, P. Roy, M.L. Yarmush, M. Toner, Effects of oxygenation and flow on the viability and function of rat hepatocytes cocultured in a microchannel flat-plate bioreactor, Biotechnol Bioeng 73(5) (2001) 379-89.
[26] Y. Kono, S. Yang, E.A. Roberts, Extended primary culture of human hepatocytes in a collagen gel sandwich system, In Vitro Cell Dev Biol Anim 33(6) (1997) 467-72.
[27] J.C. Dunn, R.G. Tompkins, M.L. Yarmush, Long-term in vitro function of adult hepatocytes in a collagen sandwich configuration, Biotechnol Prog 7(3) (1991) 237-45.
[28] A. Dash, M.B. Simmers, T.G. Deering, D.J. Berry, R.E. Feaver, N.E. Hastings, T.L. Pruett, E.L. LeCluyse, B.R. Blackman, B.R. Wamhoff, Hemodynamic flow improves rat hepatocyte morphology, function, and metabolic activity in vitro, Am J Physiol Cell Physiol 304(11) (2013) C1053-63.
[29] L.P.M. Duivenvoorde, J. Louisse, N.E.T. Pinckaers, T. Nguyen, M. van der Zande, Comparison of gene expression and biotransformation activity of HepaRG cells under static and dynamic culture conditions, Sci Rep 11(1) (2021) 10327.
[30] B. Vinci, C. Duret, S. Klieber, S. Gerbal-Chaloin, A. Sa-Cunha, S. Laporte, B. Suc, P. Maurel, A. Ahluwalia, M. Daujat-Chavanieu, Modular bioreactor for primary human hepatocyte culture: medium flow stimulates expression and activity of detoxification genes, Biotechnol J 6(5) (2011) 554-64.
[31] M.B. Esch, J.M. Prot, Y.I. Wang, P. Miller, J.R. Llamas-Vidales, B.A. Naughton, D.R. Applegate, M.L. Shuler, Multi-cellular 3D human primary liver cell culture elevates metabolic activity under fluidic flow, Lab Chip 15(10) (2015) 2269-77.
[32] X. Wang, X. Fang, J. Zhou, Z. Chen, B. Zhao, L. Xiao, A. Liu, Y.S. Li, J.Y. Shyy, Y. Guan, S. Chien, N. Wang, Shear stress activation of nuclear receptor PXR in endothelial detoxification, Proc Natl Acad Sci U S A 110(32) (2013) 13174-9.
[33] L. Burton, P. Scaife, S.W. Paine, H.R. Mellor, L. Abernethy, P. Littlewood, C. Rauch, Hydrostatic pressure regulates CYP1A2 expression in human hepatocytes via a mechanosensitive aryl hydrocarbon receptor-dependent pathway, Am J Physiol Cell Physiol 318(5) (2020) C889-C902.
[34] R. Baudoin, G. Alberto, A. Legendre, P. Paullier, M. Naudot, M.J. Fleury, S. Jacques, L. Griscom, E.

Leclerc, Investigation of expression and activity levels of primary rat hepatocyte detoxication genes under various flow rates and cell densities in microfluidic biochips, Biotechnol Prog 30(2) (2014) 401-10.
[35] A. Bader, N. Fruhauf, M. Tiedge, M. Drinkgern, L. De Bartolo, J.T. Borlak, G. Steinhoff, A. Haverich, Enhanced oxygen delivery reverses anaerobic metabolic states in prolonged sandwich rat hepatocyte culture, Exp Cell Res 246(1) (1999) 221-32.
[36] P.P. Poyck, G. Mareels, R. Hoekstra, A.C. van Wijk, T.V. van der Hoeven, T.M. van Gulik, P.R. Verdonck, R.A. Chamuleau, Enhanced oxygen availability improves liver-specific functions of the AMC bioartificial liver, Artif Organs 32(2) (2008) 116-26.
[37] H.S. Frank, M.W. Evans, Free Volume and Entropy in Condensed Systems III. Entropy in Binary Liquid Mixtures; Partial Molal Entropy in Dilute Solutions; Structure and Thermodynamics in Aqueous Electrolytes, The Journal of Chemical Physics 13(11) (1945) 507-532.
[38] I.J. Onakpoya, C.J. Heneghan, J.K. Aronson, Post-marketing withdrawal of 462 medicinal products because of adverse drug reactions: a systematic review of the world literature, BMC Med 14 (2016) 10.
[39] K. Fujimoto, H. Kishino, T. Yamoto, S. Manabe, A. Sanbuissho, In vitro cytotoxicity assay to evaluate the toxicity of an electrophilic reactive metabolite using glutathione-depleted rat primary cultured hepatocytes, Chemico-Biological Interactions 188(3) (2010) 404-411.
[40] D.F.G. Hendriks, T. Hurrell, J. Riede, M. van der Horst, S. Tuovinen, M. Ingelman-Sundberg, Mechanisms of chronic fialuridine hepatotoxicity as revealed in primary human hepatocyte spheroids, Toxicol Sci (2019).
[41] J.C. Fernandez-Checa, P. Bagnaninchi, H. Ye, P. Sancho-Bru, J.M. Falcon-Perez, F. Royo, C. Garcia-Ruiz, O. Konu, J. Miranda, O. Lunov, Advanced preclinical models for evaluation of drug-induced liver injury–consensus statement by the European Drug-Induced Liver Injury Network [PRO-EURO-DILI-NET], Journal of Hepatology 75(4) (2021) 935-959.
[42] D.G. Nguyen, J. Funk, J.B. Robbins, C. Crogan-Grundy, S.C. Presnell, T. Singer, A.B. Roth, Bioprinted 3D primary liver tissues allow assessment of organ-level response to clinical drug induced toxicity in vitro, PloS one 11(7) (2016) e0158674.
[43] S.S. Bale, S. Geerts, R. Jindal, M.L. Yarmush, Isolation and co-culture of rat parenchymal and non-parenchymal liver cells to evaluate cellular interactions and response, Sci Rep 6 (2016) 25329.
[44] A. Baze, C. Parmentier, D.F.G. Hendriks, T. Hurrell, B. Heyd, P. Bachellier, C. Schuster, M. Ingelman-Sundberg, L. Richert, Three-Dimensional Spheroid Primary Human Hepatocytes in Monoculture and Coculture with Nonparenchymal Cells, Tissue Eng Part C Methods 24(9) (2018) 534-545.
[45] Y.B. Kang, T.R. Sodunke, J. Lamontagne, J. Cirillo, C. Rajiv, M.J. Bouchard, M. Noh, Liver sinusoid on a chip: Long-term layered co-culture of primary rat hepatocytes and endothelial cells in microfluidic platforms, Biotechnol Bioeng 112(12) (2015) 2571-82.
[46] P. Paixão, L.F. Gouveia, J.A. Morais, Prediction of the human oral bioavailability by using in vitro and in silico drug related parameters in a physiologically based absorption model, International journal of pharmaceutics 429(1-2) (2012) 84-98.
[47] T. Hou, Y. Li, W. Zhang, J. Wang, Recent developments of in silico predictions of intestinal absorption and oral bioavailability, Combinatorial Chemistry & High Throughput Screening 12(5) (2009) 497-506.
[48] S. Harloff-Helleberg, L.H. Nielsen, H.M. Nielsen, Animal models for evaluation of oral delivery of biopharmaceuticals, Journal of Controlled Release 268 (2017) 57-71.
[49] S.M. Badr-Eldin, H.M. Aldawsari, S. Kotta, P.K. Deb, K.N. Venugopala, Three-Dimensional In Vitro

Cell Culture Models for Efficient Drug Discovery: Progress So Far and Future Prospects, Pharmaceuticals 15(8) (2022) 926.
[50] T. Inagaki, M. Choi, A. Moschetta, L. Peng, C.L. Cummins, J.G. McDonald, G. Luo, S.A. Jones, B. Goodwin, J.A. Richardson, Fibroblast growth factor 15 functions as an enterohepatic signal to regulate bile acid homeostasis, Cell metabolism 2(4) (2005) 217-225.
[51] Y.I. Wang, C. Oleaga, C.J. Long, M.B. Esch, C.W. McAleer, P.G. Miller, J.J. Hickman, M.L. Shuler, Self-contained, low-cost Body-on-a-Chip systems for drug development, Exp Biol Med (Maywood) 242(17) (2017) 1701-1713.